Advances in Science and Technology Research Journal

Advances in Science and Technology Research Journal, 2025, 19(7), 1–24
https://doi.org/10.12913/22998624/202413
ISSN 2299-8624, License CC-BY 4.0

Received: 2025.01.22
Accepted: 2025.05.08
Published: 2025.05.25

Evaluation of the behavior of reinforced concrete above-ground tanks subjected to blast loading

Majid Alipour[1], Mojtaba Hosseini[2*], Hamidreza Babaali[2], Mehdi Raftari[2], Reza Mahjoub[2]

[1] Department of Civil Engineering, Khorramabad Branch, Islamic Azad University, Khorramabad, Iran
[2] Department of Civil Engineering, Lorestan University, Khorramabad, Iran
* Corresponding author's e-mail: hosseini.m@lu.ac.ir

ABSTRACT

This study investigated the blast effect on hoop stresses and displacements created on the wall of over-ground reinforced concrete water tanks and the effects of blast waves, as well as the water structure interaction using ABAQUS software. Therefore, the main goal of this research was to investigate the behavior of the above-ground tanks under the effect of blast loads, taking into account the geometric characteristics, power of blast and the distance between the explosive materials and the tank. For this purpose, the main variables in the current research included the geometrical shape of the cross section of the concrete tank (circle and square with equivalent area), the amount of explosive materials (500 and 1000 kg) and the distance of explosive materials from the tank (10 and 25 meters). Also, the responses studied include maximum von Mises stress, maximum displacement created in the tank, kinetic energy and failure index. The obtained results show that by changing the cross section of the tank from circular to square, the responses of maximum von Mises stress were increased by 9.1%, maximum displacement was increased by 35.9%, kinetic energy was decreased by 6.43% and failure index was increased by 3.7% respectively. Also, the results show that by increasing the amount of explosive substance, the responses of maximum stress, maximum displacement, kinetic energy and failure index were increased by 33%, 44.4%, 6.55% and 13.3% respectively. Other results show that by a 15-meter decrease in the distance of the explosive material from the tank, the responses of maximum stress, maximum displacement, kinetic energy and failure index were increased by 42.2%, 9.9%, 8.16% and 8.23% respectively.

Keywords: RC tank, blast loading, Von Mises stress, maximum displacement, kinetic energy, failure index.

INTRODUCTION

Creating convenience, comfort, and security for users are the most important goals and philosophies of designing and producing various type of structures, regardless of the type of use. Human needs vary in different situations and cover a wide spectrum. In the times such as war, drought and water shortage, fire and need to access a high-pressure water source, conditions change in such a way that the peace and life of the citizens of a city depend on providing a source and reservoir with a suitable capacity. Due to operational restrictions, it is not always possible to design and build buried or semi-buried tanks. Thus, under such conditions, construction of above-ground tanks is considered as the only available option. It should be noted that the probability of damage caused by blast loading in above-ground tanks due to not being covered is much higher compared to buried and semi-buried concrete and steel tanks. Therefore, in this research, numerical investigation and behavior of above-ground RC tanks under blast load has been studied. Today, according to the progress of cities and industries, water tanks are still part of the necessary urban and industrial facilities and it is necessary to maintain their usability after unexpected events such as earthquakes and explosions, in order to meet the needs of water supply, sanitation and firefighting.

In fact, reservoirs are one of the important structures in the storage of fluid for storage and use in transmission networks, which usually have fix shapes in plan and height. They are designed and calculated according to input flow rate, construction site conditions as well as the type of static and dynamic loads. Therefore, a detailed investigation of the behavior of tanks under the blast load is highly essential to be studied. Thus, by accurately identifying the behavior of an important structure, such as an RC above-ground tank under the effect of blast load, a correct understanding of the performance of the structure exposed to blast load can be achieved. This knowledge ultimately leads to identifying the weak points of the structure. By strengthening and covering the weak points of the structure, an ideal engineering design can be achieved, which can ensure the safety of the structure and reduce the financial and life losses of the structure in crisis situations. The most important variables affecting the behavior of RC above-ground tanks that were considered in this study are: geometrical shape of the cross-section, the amount of explosive materials and the distance of the explosive materials from the tank.

RC above-ground water tanks are usually built in cylindrical and rectangular cube shapes, although they can be built in any beautiful and appropriate geometric shape. In general, cylindrical tanks are superior to rectangular cubic ones in terms of technical and passive defense considerations. In the areas where the soil load factor is suitable, bowl tanks are also a suitable option for large volumes. From the view point of exploitation and passive defense, tanks are usually considered as twins. However, in the absence of special limitations, the most suitable geometric dimensions for rectangular cubic tanks are obtained in terms of economy where the ratio of the length to the width of the tank is 3 to 2. In twin cylindrical tanks, the most suitable mode is to use two independent tanks with equal volume. In practice, in order to save money and time for the analysis and design of tanks, codes and analytical relationships are used. These regulatory relationships are mainly based on mechanical models. The famous mechanical models are:

- two-mass model of Housner,
- three-mass model of Haroun,
- simple method of Malhotra.

With an approximate method, Hausner calculated the dynamic effects of the fluid in a cylindrical or rectangular solid tank under the effect of horizontal motion of earthquake. He divided the hydrodynamic pressure into pulsating and fluctuating parts. The pulsating pressure is created by the coordinated movement of a part of a fluid inside the tank continuously with the solid tank, and the fluctuating pressure is created by the movement of the other part of the fluid on its free surface. Figure 1 shows the two lumped-mass model used for the rigid base-isolated tank. The upper liquid mass is denoted by convective mass (m_c) and the lower as impulsive mass (m_i) which is in rigid contact with the tank wall. The tank is assumed to move as a rigid body, with the bottom and wall undergoing the same acceleration; the impulsive mass exerts a maximum horizontal force directly proportional to the maximum acceleration of the tank bottom. The acceleration also induces oscillations in the liquid mass, causing additional dynamic pressures on the walls. The m_i predominately contributes to the base shear in the tank wall. In this model, the m_c of the liquid is considered to be connected to the solid tank wall with stiffness (K_c) at a height of H_c, and the m_i is connected rigidly to the tank wall at a height of H_i. The m_c and m_i masses are expressed in terms of total mass of liquid (M) column in the tank. The

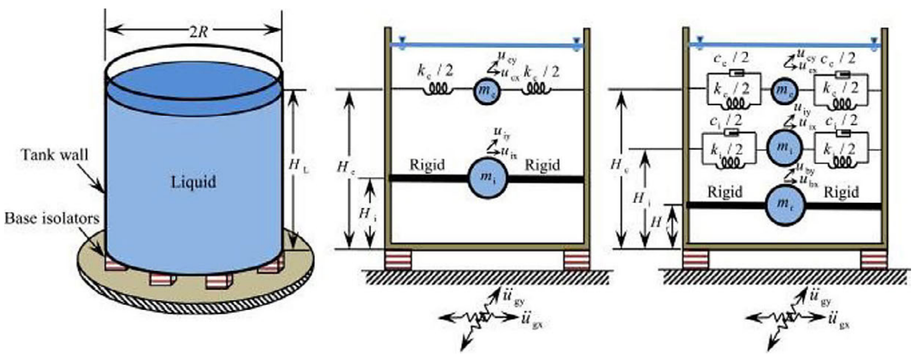

Figure 1. Mechanical lumped-mass idealization of base-isolated tanks [2]

detailed parameters of this model are given by Housner. The main difference between Haroun's proposed model and Housner's model is that in Housner's model, a rigid wall is assumed, while in Haroun's model ductile wall is considered. The model proposed by Malhotra is based on code relations. In this method, two periods are presented for the pulsating and fluctuating part, with difference that the effects of other modes are combined with these two main modes [1].

Rectangular and circular RC tanks with fix and flexible foundations, as well as air tanks with supporting foundations are considered at ACI350.3. In NZSEE code, circular and rectangular concrete ground tanks with rigid and flexible foundations, as well as concrete air tanks are considered and evaluated. In Eurocode 8, circular and rectangular tanks with girder base and air tanks have been evaluated. Also, in Iranian code named publication 123, RC circular and rectangular concrete tanks as well as concrete air tanks were analyzed and investigated. Therefore, it can be seen that a large percentage of the mentioned codes are related to RC tanks. Different codes have presented various relationships in order to calculate the period time of tanks under different conditions [3]. Explosion is a very rapid release of energy in the form of light, heat, sound and shock waves. When an explosion occurs, energy is released suddenly and in a very short time (a few milliseconds) and the effect of this energy is seen in the form of thermal radiation and propagation of waves in space. Explosives are classified according to their material state into solid, liquid and gas types, usually the solid type is more useful in bombs and produces stronger waves. In terms of excitability and reaction initiation, they are divided into primary and secondary types, where the primary type reacts quickly and due to the smallest stimulus such as a spark or shock [4].

Jacobsen focused his studies on cylindrical tanks with a rigid wall and Hausner modeled the rigid cylindrical and rectangular tanks system in a form that has practical application for civil engineers. In Hausner's model, liquid pressure is divided into two parts. The first one is impact parts which is caused by a part of the liquid that has an acceleration equal to the wall acceleration and the second one is transfer part which is caused by the liquid sway movement. Epstin determined the maximum forces caused by an earthquake by presenting a series of equations and tables assuming that the transfer component acts in the upper part of the liquid [5]. In 2010 and 2011, Ghaemmaghami and Kianoush investigated the dynamic behavior of rectangular ground concrete tanks using finite element method in two and three dimensions. In other studies, dynamic analysis of the RC tanks was performed using the finite element method with modal and time-history analysis and the effect of different elements on the dynamic responses was investigated [6, 7, 14, 15]. Khoshmood et al. [8] analyzed the sensitivity of retrofitting buried concrete tanks and the effect of soil type and distance from the explosion site. They used a soil model of 100-meter length and 50-meter width. They used Drucker-Prager model in their study. The results of the study show that the explosive response of the buried tank is highly sensitive to the characteristics of the location and site of the structure. On the basis of the elastic and plastic parameters, as the soil soften, the displacement and stress created in the tank wall increases, so that the stress and displacement in the tank wall in soft soil compared to stiff soil are 62% and 42% higher, respectively. In the other words, the behavior of concrete tank buried in less stiff soil is more critical and building a tank in a soft soil should be avoided. In 2017, Lin and Li [9] investigated the performance of RC tanks under sever seismic excitation. They evaluated the safety of the structure based on two specific limit state, including serviceability limit state and ultimate limit state. The results obtained from their numerical analysis showed that the concrete tanks are placed in the serviceability state for acceleration record with PGA equal to 0.8–1.1, and for PGA in the range of 1.2–1.7, it passes the ultimate state. Peyman and Shabdiz [10] investigated the effect of explosion on above-ground floating roof tanks. Explosive loading was investigated in their study on two widely used tank samples with two types of floating roof. The nonlinear dynamic analysis of the structure under the effect of load caused by the explosion was carried out using a numerical method for 30 different cases of the explosive loads. The explosions on two types of tanks are modeled by the Air Blast model in the software and analyzed based on Brad relations. In this way, when the explosion occurs, more pressure is applied to the body of the tank. The explosion scenarios applied to the tanks are based on the two parameters of the distance and the amount of the explosive charge. The distance was assumed to be 5, 15 and 25 meters from the closest point of the tank body to the source of the explosion. The amount of explosive charge according to the type of attack in 5 cases, the weight of the explosive TNT equal to the values of 5, 20, 100, 500 and 1000 kg was considered. The results show that the investigated tank body is vulnerable to some explosive loading scenarios and will be damaged based on the standard failure criteria of API650. In the following, suggestion to prevent economic and environmental losses as well as necessary measure such as retrofitting, passive defense and crisis management after destruction were discussed. The summary of the results obtained from their study can be expressed as follows:

- among the two types of tanks presented in their study, the tank with a diameter of 50 meters compared to the tank with a diameter of 32 meters, has a more suitable behavior in terms of absorbing and dissipating energy. Because the larger tank has more liquid volume, ca dissipates the energy with favorable conditions.
- the pressure on the elements of the tank decreases with the distance from the explosion site, with the second power of the distance.
- the behavior of the tank is very sensitive at a distance of about 5 meters, and up to this distance, explosions of less than 5 kg can be tolerated. As a result, above-ground tanks are relatively resistant to light terrorist attacks.

In 2014, Burkacki et al. [11] investigated the seismic behavior of steel tanks using a shaking table test. According to laboratory limitations of tank sample, it was converted to the scale of 1 to 33.33, the diameter and height of the tank were 1.5 and 0.7 meters respectively. The weight of the tank was 86 kg, the thickness of the bottom plate and roof were 3 and 1.2 mm, respectively. The tested tank was examined for four states: empty, filled of water up to the height of 162 mm, filled of water up to the height of 324 mm and filled of water up to the height of 486 mm. in all cases it was investigated under the earthquake records of Suwalki, El Centro and Polcois Minigtermore.

After that, the recorded signals were subjected to data processing and analysis using a computer program. Then, the results of the response of the structure were provided in the form of an acceleration-time diagram under the mentioned earthquakes. According to the results, the response of the structure has increased in the form of time acceleration in a tank that is completely full.

Despite the considerable amount of studies conducted regarding the analysis and evaluation of the behavior of RC tanks against the application of various types of loading [12, 13], until now, a comprehensive has not been conducted regarding the analysis and evaluation of the behavior of above-ground RC tanks against the blast loads, especially it has not been carried out with consideration of geometric characteristics of the tank section. Therefore, in this study, the behavior of two circular and square RC tanks for two amounts of explosives and at two different distances from explosion site was investigated and evaluated. In 2024, Santoso et al. [16] studied the dynamic soil-structure interaction on the seismic behavior of RC base-isolated buildings. Also in 2024, Li et al. [17] studied seismic optimization design tank structure.

METHODS AND MATERIALS

Finite element (FE) modeling of the tank

According to the title of the study, which is Evaluation of the behavior of reinforced concrete above-ground tanks subjected to blast loading, the steps of the research can be described as follows:

Modeling of two categories of square and circular above-ground RC tanks in Abacus environment: in this step a square tank with the ratio of length to height (L/H) equal to 2 was modeled using abacus finite element software. Also, a circular cross section tank was modeled with the ratio of diameter to the height (D/H) of 2.25.

Applying different loading scenarios caused by explosion in Abacus software to the model built in the previous stage using the ConWep method: at this stage, each of the primary models was subjected to explosive loading for different amounts of explosive material (2 numerical values) and different distances (2 distinct distances) from the explosion site (totally 4 different states).

In order to ensure the correctness of considered models, the verification process was done using the results of another research. After validation, the results were evaluated in different modeling modes and compared with each other. In this study, the validation was done based on one of the models studied by Ghaemmaghami and Kianoush [6]. It should be noted that the responses studied in this study are:

- stress contours created in above-ground RC tanks under the effect of blast load.
- displacement created in above-ground RC tanks under the effect of blast load.

- diagrams of distributed energy in above-ground RC tanks for explosive loading.
- Park-Ang failure index.

It should be mentioned that the stiffness of the soil is considered infinite in the present study and the effects of soil-structure interaction are practically neglected. Also, the variable used can be introduced as follows:

Geometry of above-ground tank: one of the variables in the current study is the geometry of above-ground tank. The cross-sectional shape of the tank and the height of the structure were considered as two geometrical variables. Therefore, the RC tank was studied and evaluated in two circular and square geometries with a cross-sectional area of equal to 900 m^2, in such a way that the dimensions of the cross-section of square tank were equal to 30 m and its height was equal to 15 m. Thus, for square tank, the ratio of the length to the height (L/H) was equal to 2. Also, in the case of tank with a circular cross-section, the ratio of the diameter to the height of the tank (D/H) was equal to 2.25 (in this case, the diameter of the tank was equal to 33.85 m and the height of the tank was equal to 15 m). Amount of explosive material: as it was mentioned before, the loading studied here was the explosive loading type. Therefore, one of the effective factors in causing damage was the magnitude of the force caused by the explosion and the amount of explosive material was one of the variables. Two numerical values of 500 kg and 1000 kg of explosive were used in this study. Blasting distance from the tank: the blasting distance from the tan was one of the other considered variables. The closer the explosion site is to the structure, the higher the probability of failure and damage in the studied structure. The distances investigated in this study included 10 and 25 meters.

In the present study, FEM was used for the analysis of the base-isolated liquid storage tank of radius, R and liquid height, H as shown in Fig. 2. The water contained in the tank was modeled using the eight-node 3-D continuum acoustic element AC3D8R with reduced integration and hourglass control, for acoustic wave propagation having only pressure degree-of-freedom at each node. The flexible tank walls were modeled using the four-node quadrilateral and triangular 3-D shell elements S4R and S3R, respectively, with reduced integration and hourglass control, as shown in Figure 2. The rigid tank wall was modeled using the shell elements same as that for flexible tank wall, but a very large modulus of elasticity of the shell material was assigned to account for tank rigidity. Thus, a modulus of elasticity twenty times greater than flexible shell material was used. The interaction between the tank wall and acoustic liquid elements was defined using a surface-based tie constraint. The acoustic surface in the constraint was designated to be the slave surface; the tank internal surface was defined as the master surface.

On the tank walls, 532 grade-22 rebars are perpendicular, and in every 1 m height, 5 grade-16 rebars circularly surround the vertical rebars. These bars are buried inside the concrete. For a square tank, 601 grade-22 rebars are perpendicular. The B31 element was also used to model vertical and hoop rebars in ABAQUS.

Coupled Euler-Lagrange formula

The coupled Euler-Lagrange (CEL) formula analysis allows modeling of the Euler-Lagrange interaction domains in one model. This analysis is typically used to model the interactions of a solid and a fluid. Therefore, in the CEL method, the

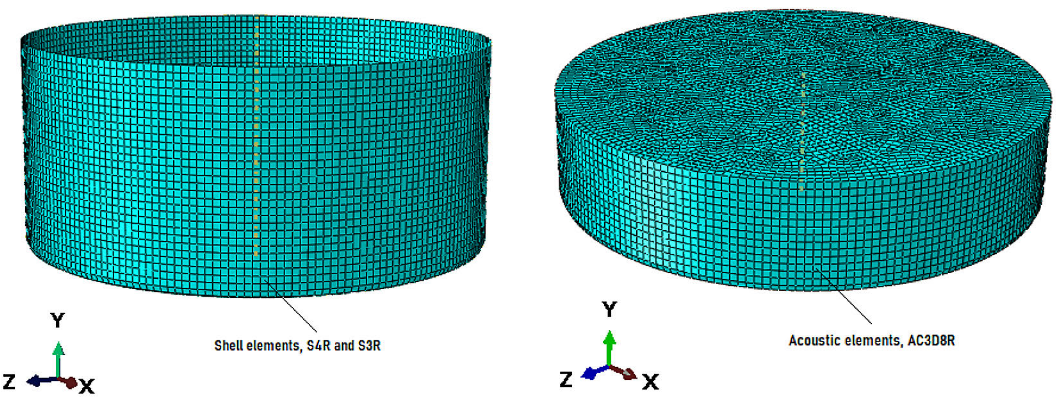

Figure 2. Finite element (FE) model of cylindrical liquid storage tank

Euler material can contact the Lagrange, known as the Euler-Lagrange contact. Therefore, this powerful tool makes it possible to model many multi-phase problems, including fluid-structure contact. Because of Eulerian fluid modeling, the problems caused by large deformations of the fluid have been eliminated. In this method, the fluid elements are fixed in the space, and the fluid flows smoothly inside them; the water tank structure is defined in this method as the Lagrangian formulation. Since the implementation of the Euler method in ABAQUS software is based on the fluid volume method, in this method, the position of the Euler material in the mesh environment is determined by calculating the volume fractions of Euler in each element. By this definition, if an element is filled with a substance, its Euler volume fraction is one, and if no substance is included in it, its Euler volume fraction is zero [18].

Fluid properties in ABAQUS

In turbulence issues, the fluid can be considered incompressible and non-viscous. A practical method for fluid modeling in ABAQUS/explicit is to use the Newtonian shear viscosity model and the U_S-U_P linear equation. The bulk functions act as correction parameters for fluid incompressibility constraints. Since the turbulence of the fluid inside the water tank is free and unconstrained, the bulk modulus can be considered two to three times smaller than the actual value, and the fluid can still behave in an incompressible way. The shear viscosity acts as a corrective parameter to neutralize the shear modes that cause mesh failure. Because water is a non-viscous fluid, the shear viscosity of the fluid must be considered small. High shear viscosity results in highly rigid responses. The value of suitable viscosity can be calculated based on the value of the bulk modulus [18].

Energy equation and Hugoniot curve

The energy equation in the absence of heat transfer is written as Equation 1:

$$\rho\frac{\partial E_m}{\partial t} = (P - P_{bv})\frac{1}{\rho}\frac{\partial \rho}{\partial t} + S\colon \dot{e} + \rho\dot{Q} \qquad (1)$$

where: P is the pressure; P_{bv} is the pressure due to the viscosity of the fluid; S is the deviatoric stress tensor; $\dot{e}$ is the deviatoric part of the strain rate; $\dot{Q}$ is the heat rate per unit mass, and E_m is the internal energy per unit mass. The equation of state is a function of density ρ and internal energy per unit E_m mass. Equation 1 can define all the equilibrium states that exist in an object. Internal energy can be omitted from the above equation to obtain the relation between ρ and V or its equivalent ρ and $1/\rho$. The relationship between ρ and $1/\rho$ is called the Hugoniot curve [18].

$$P = f(\rho E_m) \qquad (2)$$

Figure 3 schematically shows the Hugoniot curve; the Hugoniot pressure P_H is only a function of density, and the curve is generally plotted by processing experimental data [18].

State equation Mie-Gruneisen

In the Mie-Gruneisen equation, the energy is linear. Its standard form is given in Equation 3:

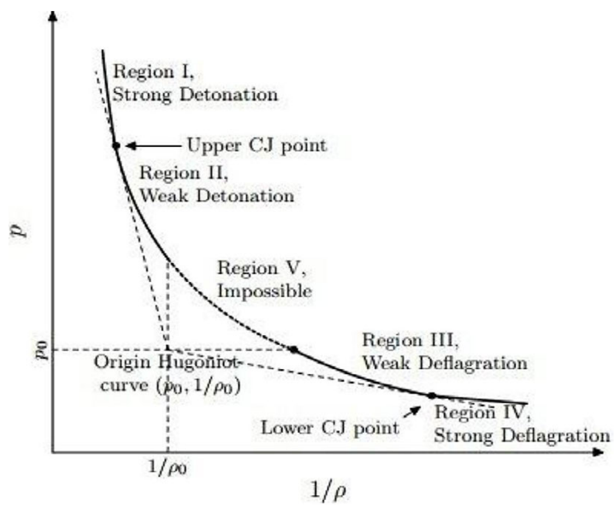

Figure 3. The Hugoniot curve for pressure-time relationship definition [18]

$\dot{Q}$

$\dot{e}$

$$P - P_H = \Gamma\rho(E_m - E_H) \tag{3}$$

where: P_H and E_H are the specific pressure and the specific energy of Hugoniot per unit mass, respectively, and is the Gruneisen coefficient. The Gruneisen coefficient is calculated using Equation 4. The specific pressure and the specific energy of Hugoniot are only functions of density.

$$\Gamma = \Gamma_0 \frac{\rho_0}{\rho} \tag{4}$$

In Equation 4, Γ_0 is the constant of matter, and ρ_0 is the reference density. The energy of Hugoniot E_H is dependent on the Hugoniot pressure and is obtained using Equation 5:

$$E_H = \frac{P_H}{2\rho_0}(1 - \frac{\rho_0}{\rho}) \tag{5}$$

By placing Equation 4 And 5 in Equation 3, the Mie-Gruneisen equation of state is obtained as Equation 6:

$$P = P_H\left(1 - \frac{\Gamma_0(1-\frac{\rho_0}{\rho})}{2}\right) + \Gamma_0\rho_0 E_m \tag{6}$$

Linear Hugoniot U_S-U_P

The P_H equation is shown by processing the Hugoniot information in Equation 7:

$$P_H = \frac{\rho_0 C_0(1 - \frac{\rho_0}{\rho})}{(1-S + \frac{S\rho_0}{\rho})^2} \tag{7}$$

In this relation, S and C_0 create a linear relationship between the U_S impulsive velocity and the U_P particle velocity according to Equation 8:

$$U_S = C_0 + SU_P \tag{8}$$

S and C_0 are the slope of the Hugoniot curve and the velocity of the sound wave in water, respectively. The velocity of the sound wave in water is calculated by Equation 9:

$$C_0 = \sqrt{\frac{K}{\rho}} \tag{9}$$

In this relation, K is the modulus of the fluid bulk. According to the ABAQUS software guide, the value of S, the slope of the curve and$\Gamma_0\Gamma_0$, and the Gruneisen coefficient for water are considered equal to zero.

The process of modeling and validation

To build a RC tank, the specific weight of the concrete is considered as 2500 kg/m^3, Poisson's ratio is 0.3 and the modulus of elasticity is 20 GPa. Steel is used to model reinforcements in concrete. Since blast loads usually produce incredibly high strain rates in the range of 100–10000 s^{-1}, they change the mechanical properties of materials in the structure and the expected mechanisms. According to Table 1, the plastic properties of the steel were assumed using the Johnson-Cook hardening model to consider the impact of strain rate on the stress. According to Equation 10, stress is defined as a function of plastic strain, strain rate and temperature in the Johnson Cook model. This feature is easily defined in the ABAQUS software.

$$\sigma = (A + B\varepsilon^n)(1 + C.Ln\varepsilon^*)(1 - T^{*m}) \tag{10}$$

$\dot{\varepsilon}$

where: ε^* is the dimensionless plastic strain rate in the reference strain rate ε_0, and $\dot{\varepsilon}$ is equal to the plastic strain rate; T^* is the corresponding dimensionless temperature; A is the initial rupture strength of steel at a plastic strain rate of $\dot{\varepsilon} = 1/s$, and the temperature is 298 Kelvin; B and n simulate the hardening behavior of steel independent of the strain rate; and C reflects the hardening behavior dependent on the strain rate; and m is the thermal softening coefficient obtained for steel from mechanical tests and is equal to 0.114. The specifications of the Johnson-Cook model for rebar are given in Table 1.

The maximum and minimum compressive stress values in the inelastic strain are 20.5 MPa and 11.5 MPa. Also, the tensile stress of concrete in the cracking strain is 0.3 MPa. After assigning the materials to the parts, the part were assembled and the size and distance of explosive material were defined using the Kanob method. Therefore, the considered points were defined as reference points using offset from point, and then the amount of explosive material was defined. It

Table 1. Johnson-Cook model specifications

Variable	Value
A (MPa)	360
B (MPa)	635
N	1.03
M	0.114
Melting temperature (K)	1500
Transition temperature (K)	298
C	0.075
Epsilon dot zero	1

should be noted that the bottom of the tank has a fixed support and is completely fixed modeled. In order to ensure the accuracy of the modeling done in the current study, the results were verified using the results presented in a scientific reference. For this purpose, one of the Ghaemmaghami and Kianoush [6] models was simulated and the results were compared. The geometry of square tank modeled for verification is shown in Figure 4. In this figure, L_x = 15 m, L_z = 30 m, H_w = 6 m, H_1 = 5.5 m and t_w = 0.6 m. In order to ensure the validity of the present results, the response investigated in this study corresponds to the changes in the response of hydrodynamic pressure along the height of the tank. Figure 5 compares the hydrodynamic pressure response of the fluid for different height of the tank with the results of Ghaemmaghami and Kianoush [6]. As it can be seen, by increasing the height of the tank, the hydrodynamic pressure of the fluid has been decreased. The maximum difference between the results of the current research and the results of reference [6] is obtained at zero height level. Also, it can be seen that the maximum hydrodynamic pressure obtained based on the study of Ghaemmaghami and Kianoush in the 11-meter tank is equal to 26 kPa. In turn, the numerical value of the hydrodynamic pressure at such depth of the tank in this study is equal to 24.8 kPa. As it can be observed in Table 2, the maximum difference between the results of this study and results of Ghaemmaghami and Kianoush was obtained at the depth of 7.3 m which is 4.7%. This insignificant difference indicates the desired accuracy of the modeling in the present study.

RESULTS AND DISCUSSION

In order to answer the research questions and achieve the goals of the study, the effect of each mentioned variable on the behavior of aboveground RC tank were investigated. In this situation other variables were considered constant. This process was repeated for each variable and the effect of all variables on the response of the structure was studied as well as evaluated. Therefore, in the following, the effect of each of the

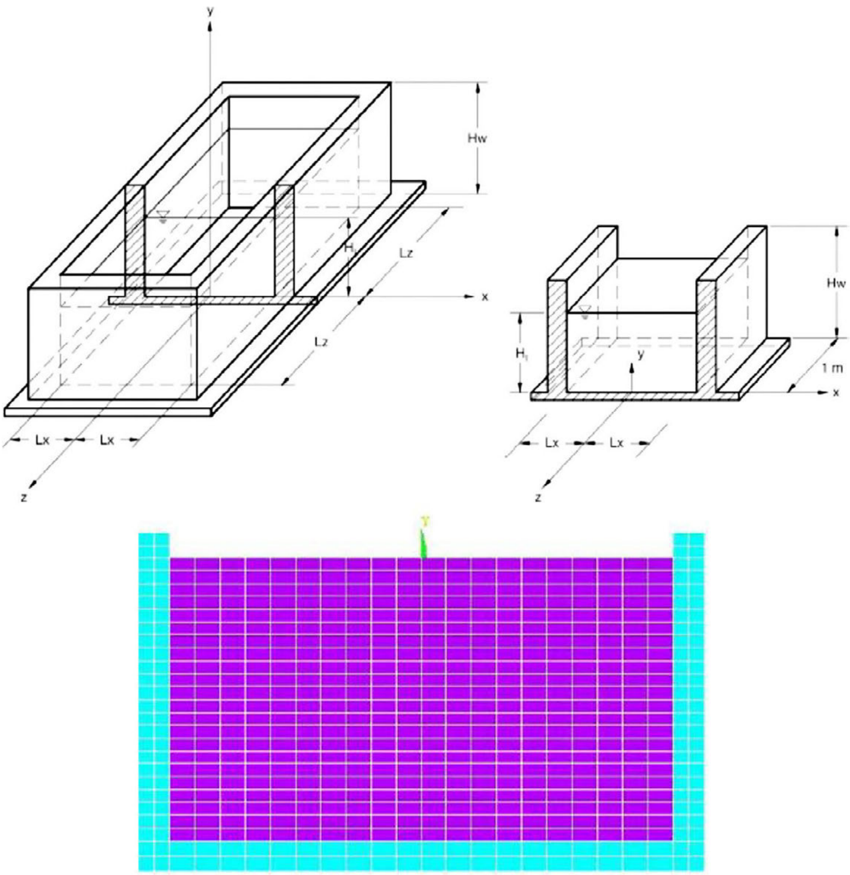

Figure 4. Schematic configuration of rectangular liquid tank and 2D finite-element model of rectangular liquid tanks [6]

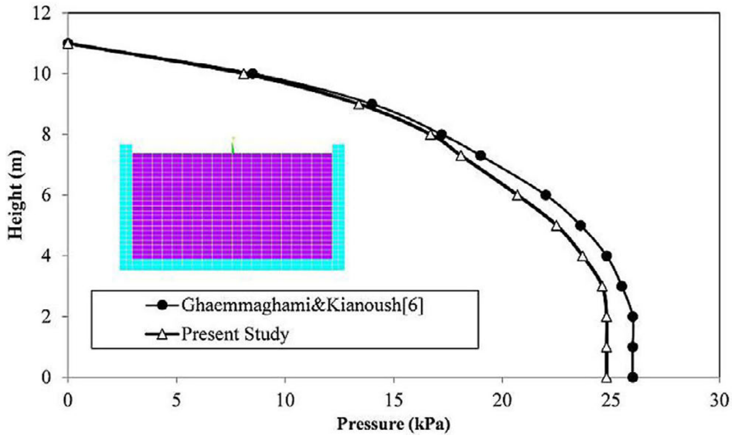

Figure 5. Comparison of the response of the hydrodynamic pressure distribution of water in the tank in this study and responses of Ghaemmaghami and Kianoush [6]

Table 2. The detailed results of verification

Pressure (kPa)	Ghaemmaghami and Kianoush [6]	This study	Difference%
Depth of 8m	17.2	16.7	2.9
Depth of 7.3	19	18.1	4.7
Depth of 0	26	24.8	4.61

variables of the geometrical shape of the section, the amount of explosive material and the distance of explosive material on the overall response of the above-ground tank under the effect of the blast load was investigated and evaluated. The scenarios studied in the current research were named according to Table 3.

Effect of geometric shape on the behavior of RC tank

In order to investigate the effect of cross-sectional geometric shape of RC tank, other variables were considered constant. Therefore, the considered variable in this case was the only geometric shape of the tank section. In the first case, the cross-section of the tank is circular and in the second case was considered square. In the circular state, the diameter of the section was equal to 33.85 m and the height of the tank was 15 m. In the square state, the length of the sides of the section were 30 m and the height of the tank was 15 m. Under these conditions, 500 kg of explosive materials placed at a distance of 25 m from the tank were used.

Figures 6 and 7 show the distributed stress in V_1 and V_2 models respectively. The only difference between these two models is the geometric shape of the tank section. It can be seen that the stress distributed in the circular section is uniform and spread on all the peripheral surface of the tank. However, if the cross-section of the tank is square, the stress concentration will be observed. In other words, if the cross-section of the tank is circular, the stress is distributed on the entire peripheral surface of the cross-section, but in the square tank, the stress is created only in the wall opposite to the explosion and the other sides of the square have not a considerable stress. The maximum stresses created in the circular and square

Table 3. Scenarios studied in the current research

Model name	Geometry of cross-section	Amount of explosive material (kg)	Distance (m)
V_1	Circular	500	25
V_2	Square	500	25
V_3	Circular	1000	25
V_4	Circular	500	10

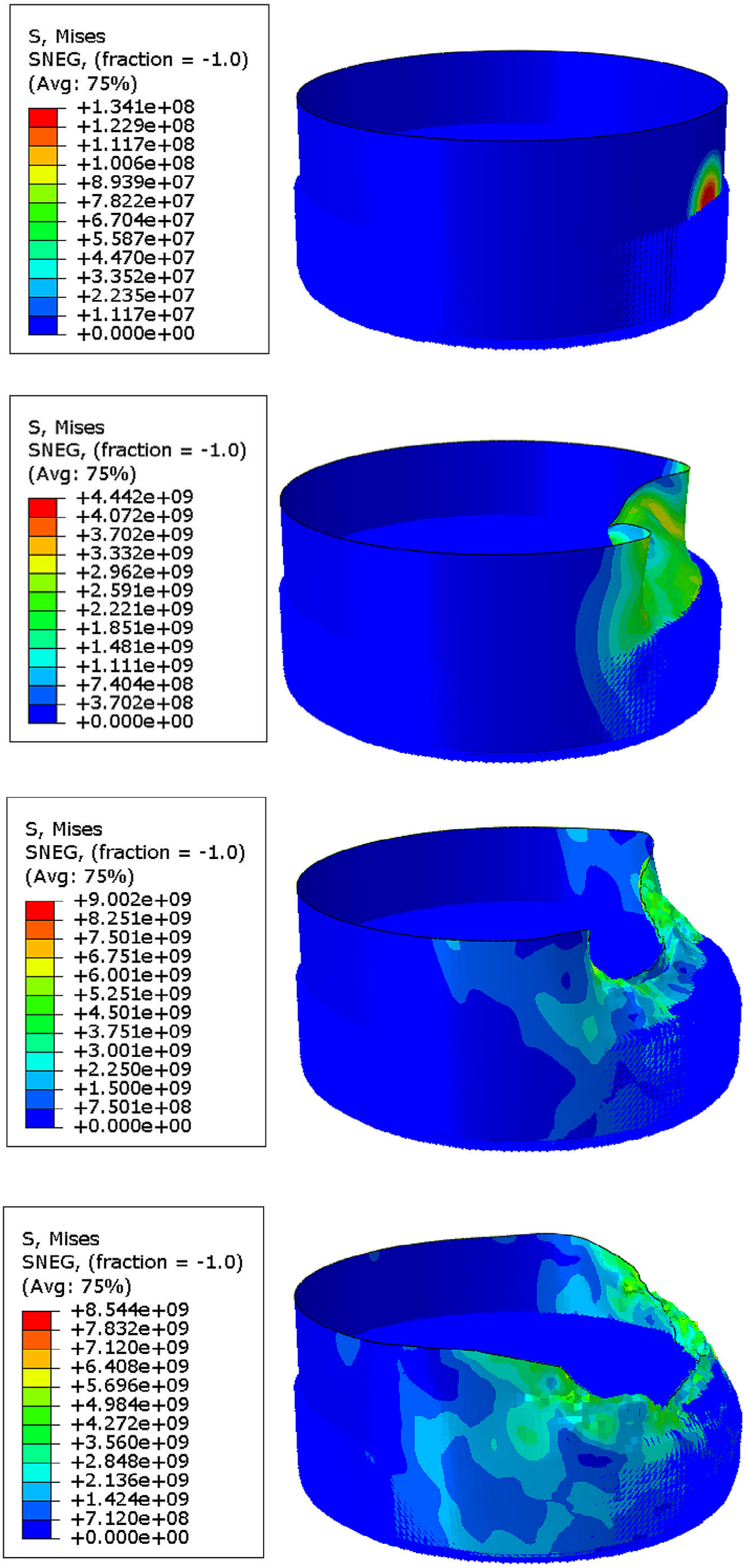

Figure 6. Von Mises stress distributed in V_1 model

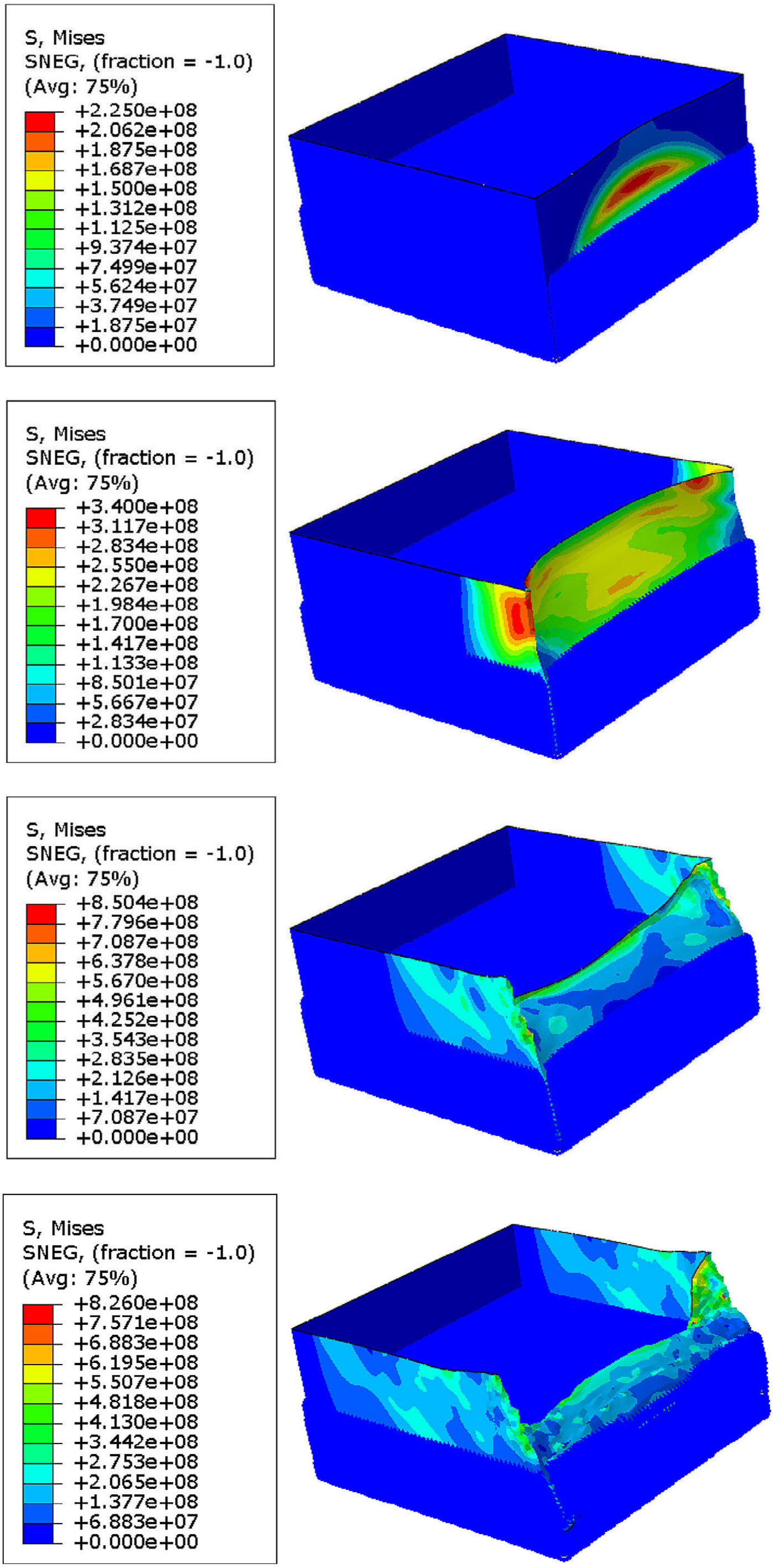

Figure 7. Von Mises stress distributed in V_2 model

sections were 590 MPa and 649 MPa respectively. Therefore, using a circular section for the tank compared to a square section will reduce the maximum stress distributed in the wall of the concrete tank by 9.1%. Figures 8 and 9 show the maximum displacement created in the V_1 and V_2 model respectively. It can be seen that the uniform stress distribution in the circular tank compared to the square section, caused the displacement created in the concrete wall of the circular tank to be less than that of the square section. The maximum displacement created in the circular and square tank is 7.5 mm and 11.7 mm respectively. Therefore, it can be seen that by changing the cross-section of the tank from circular to square, the displacement will be increased by 35.9%. Figure 10 shows the kinetic energy in V_1 and V_2 models. As it can be seen, by changing the cross-section of the RC tank from circular to square, the kinetic energy will be decreased by 6.4%. In other words, when the RC tank has circular and square cross-section, the kinetic energy in the tank is equal to 171 kJ and 160 kJ respectively. One of the most famous composite indices is Park-Ang failure index, which is considered as a linear combination of damage caused by the deformation of each member and the effects of repeated loading. This index changes between zero (not damaged) and one (complete failure).

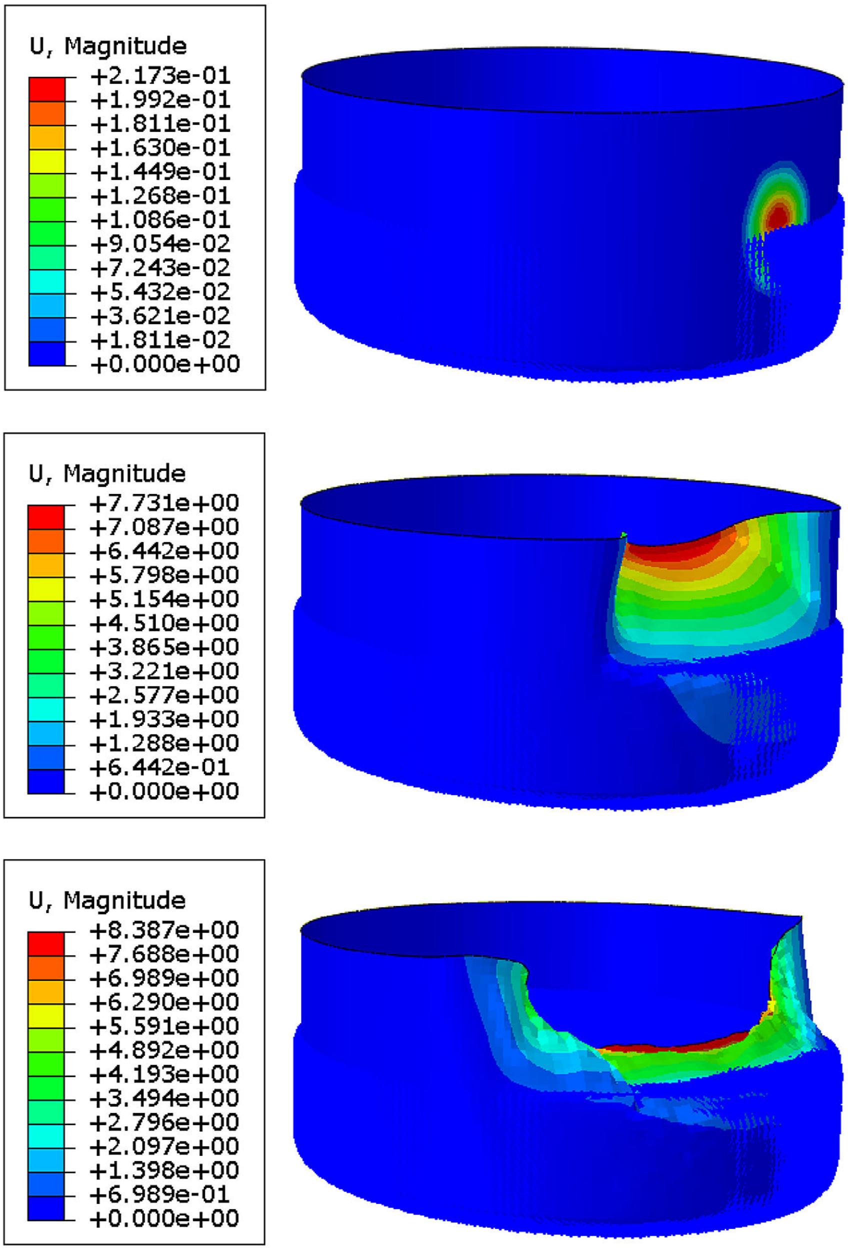

Figure 8. Displacement in V_1 model

In this study, in order to compare and understand the failure conditions in different models, the numerical values of the failure were normalized in such a way that all responses are divided by the maximum numerical value of failure. Figure 11 shows the failure index of V_1 and V_2 models. It can be seen that the failure index in the tank with a square cross-section is 3.7% more than a circular cross-section tank. This issue can be justified due to stress concentration and non-uniform distribution of stress in square compare to circular section. Therefore, the probability of damage and failure in the square section is 3.7% higher than in the circular section.

Effect of amount of explosive material on the behavior of RC tank

In order to investigate the effect of TNT explosive amount, other variables are considered constant. Therefore, the variable considered in this state is only amount of explosive material. Amount of explosive material in first and second cases are considered as 500 kg and 1000 kg, respectively. In both cases studied in this section, the cross-section of the tank is circular and the distance of the explosive material from the tank is considered to be 25 m. Figure 6 shows the stress distribution in V_1 model, and Figure 12 shows the stress distribution

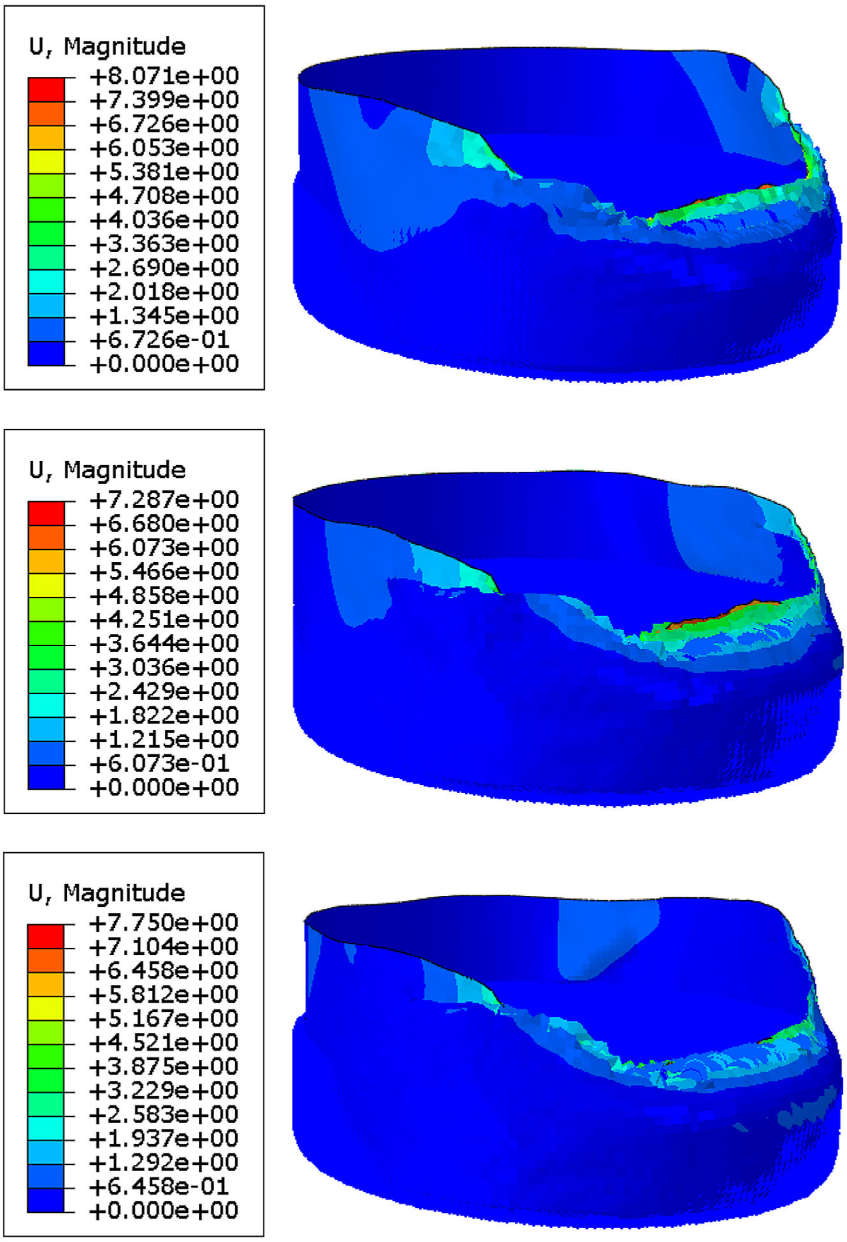

Figure 8. Cont. Displacement in V_1 model

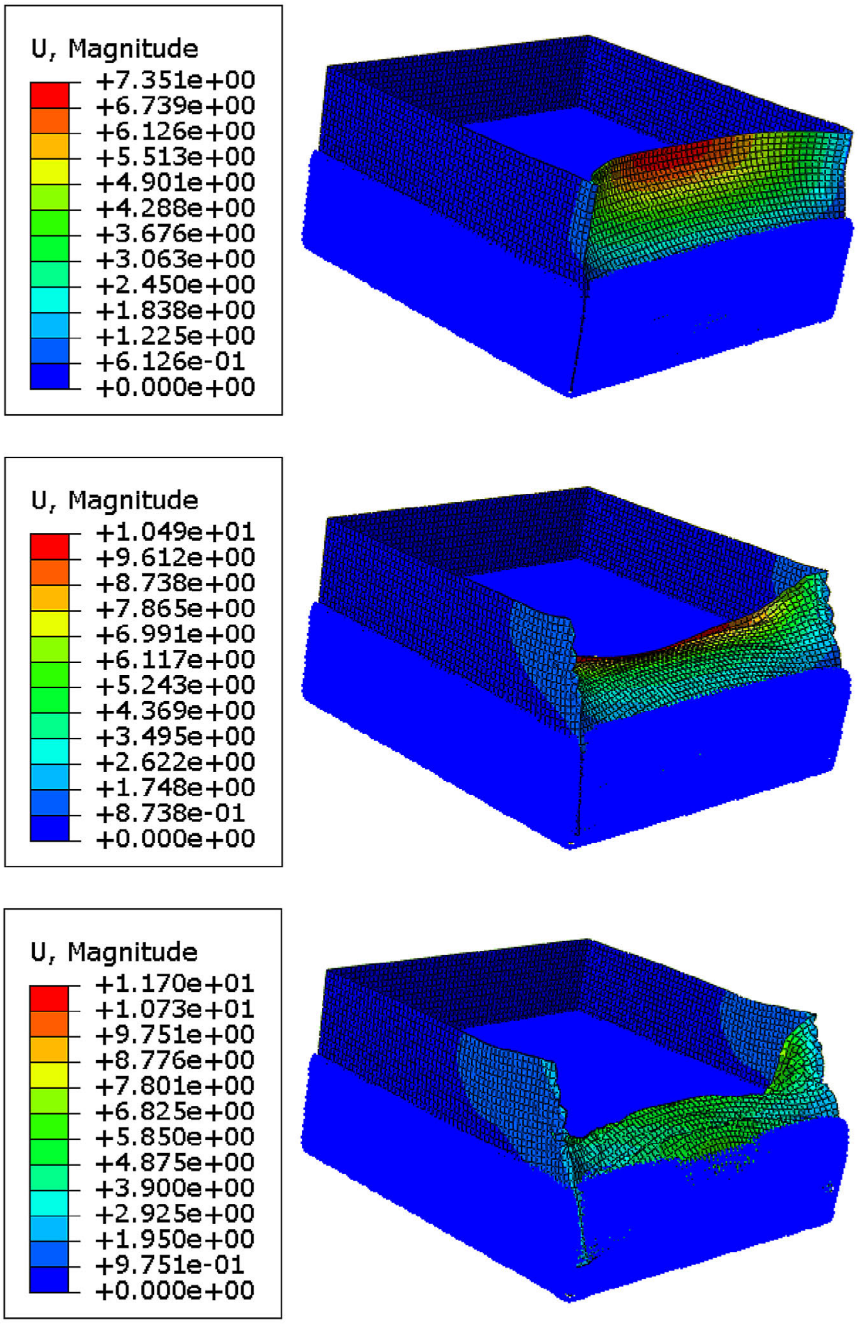

Figure 9. Displacement in V_2 model

in V_3 model. The only difference of the mentioned figures is the amount of explosive materials. As it can be seen, by increasing the amount of explosive material, maximum numerical value of the stress distributed in the wall of the RC tank will be increased. Thus, the maximum stress created in V_1 and V_3 models are 590 MPa and 881 MPa respectively. Therefore, it can be seen that with a 50% increase in the amount of explosive material, a 33% increase in the maximum stress created in the tank will be observed. Figure 8 shows the maximum displacement created in the V_1 model. Also, the displacement created in the V_3 model was shown in Figure 13. It can be observed that with a 50% increase in the explosive material, maximum displacement created in the tank wall and the displacement of the fluid inside the tank will be increased. Furthermore, it can be seen that under the explosion of 500 kg of explosives, maximum displacements created in V_1 and V_3 models are equal to 7.5 mm and 13.48 mm respectively. Also, by increasing the amount of explosive material from 500 kg to 1000 kg a 44.36% increase in the maximum displacement created in the RC tank will

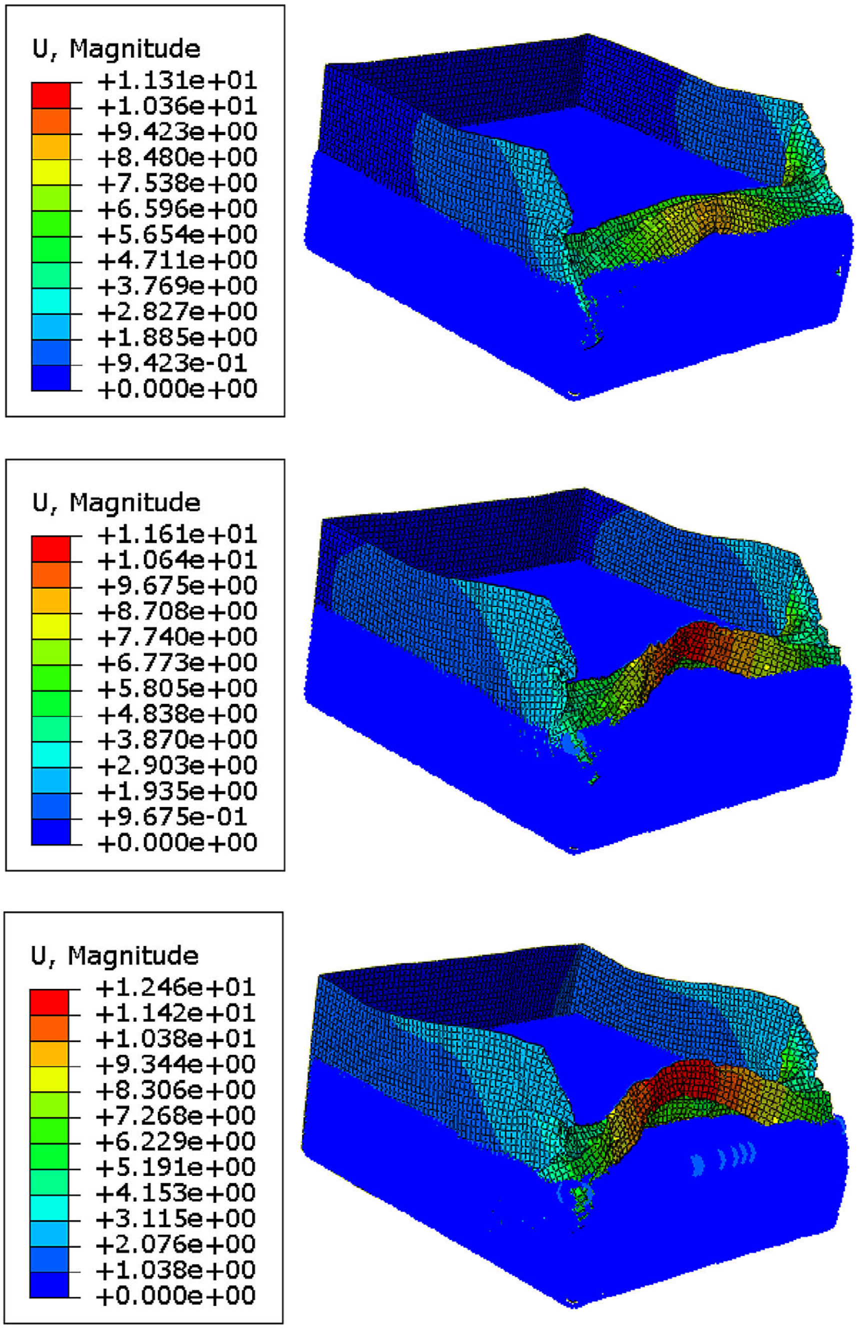

Figure 9. Cont. Displacement in V_2 model

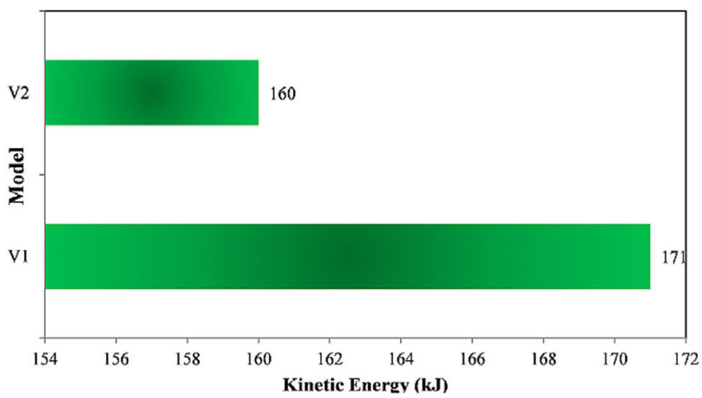

Figure 10. Effect of geometrical shape of the section on the kinetic energy response of the tank

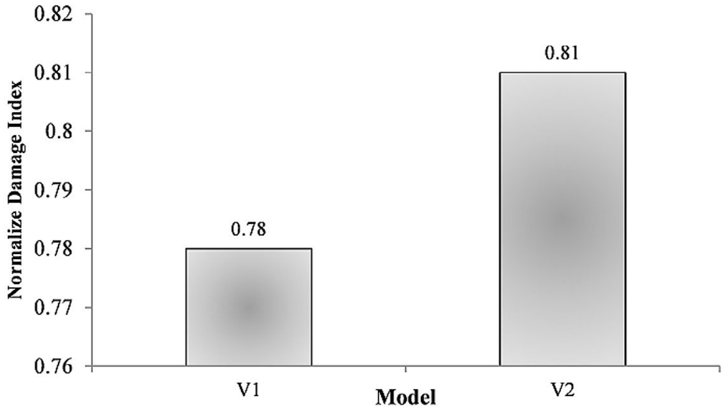

Figure 11. Effect of geometrical shape of the section on the failure index

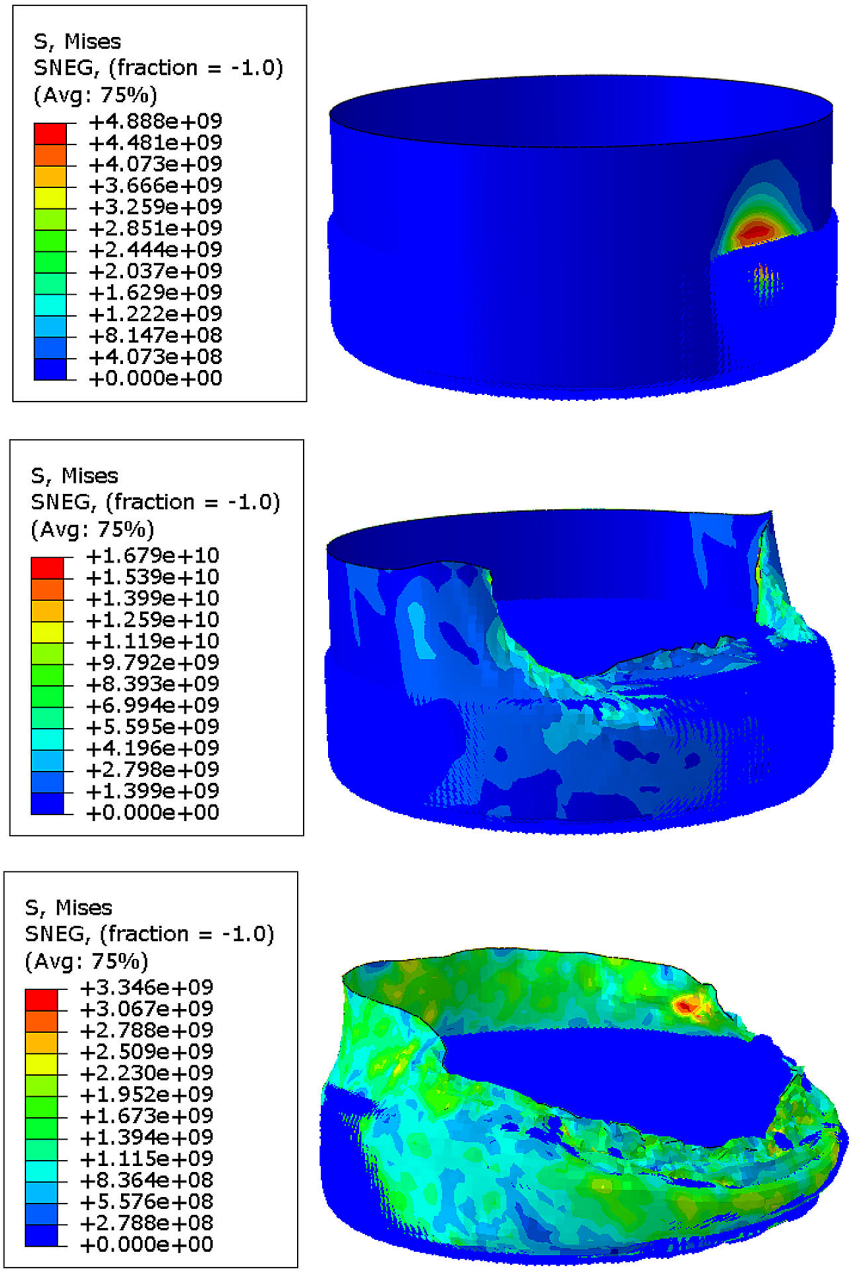

Figure 12. Von Mises stress distributed in V_3 model

occur. Figure 14 shows the recorded kinetic energy in two models of V_1 and V_3. As it can be seen, with a 50% increase in the amount of TNT explosive, the numerical value of the kinetic energy increases by 6.5%. In other words, when the concrete tank is subjected to the explosion of 500 kg and 1000 kg (with a constant in other variables) of explosive material, the kinetic energy is equal to 171 kJ and 183 kJ, respectively. In the Park-Ang failure index, the closer the numerical value of the index is to zero, the lesser the damage, and the closer the numerical value of the index is to one, the more severe the damage in the element is. Figure 15 shows the failure index of V_1 and V_3 models. It can be seen that failure index of V_3 is 13.3% more than V_1. In other words, with a 50% increase in amount of explosives, the probability of damage and failure in the RC tank structure increases by 13.3%.

Effect of distance of the explosive material on the behavior of RC tank

In order to investigate the effect of the distance of TNT explosives from the tank, other variables are considered constant. Therefore, the only considered variable in this case will be the

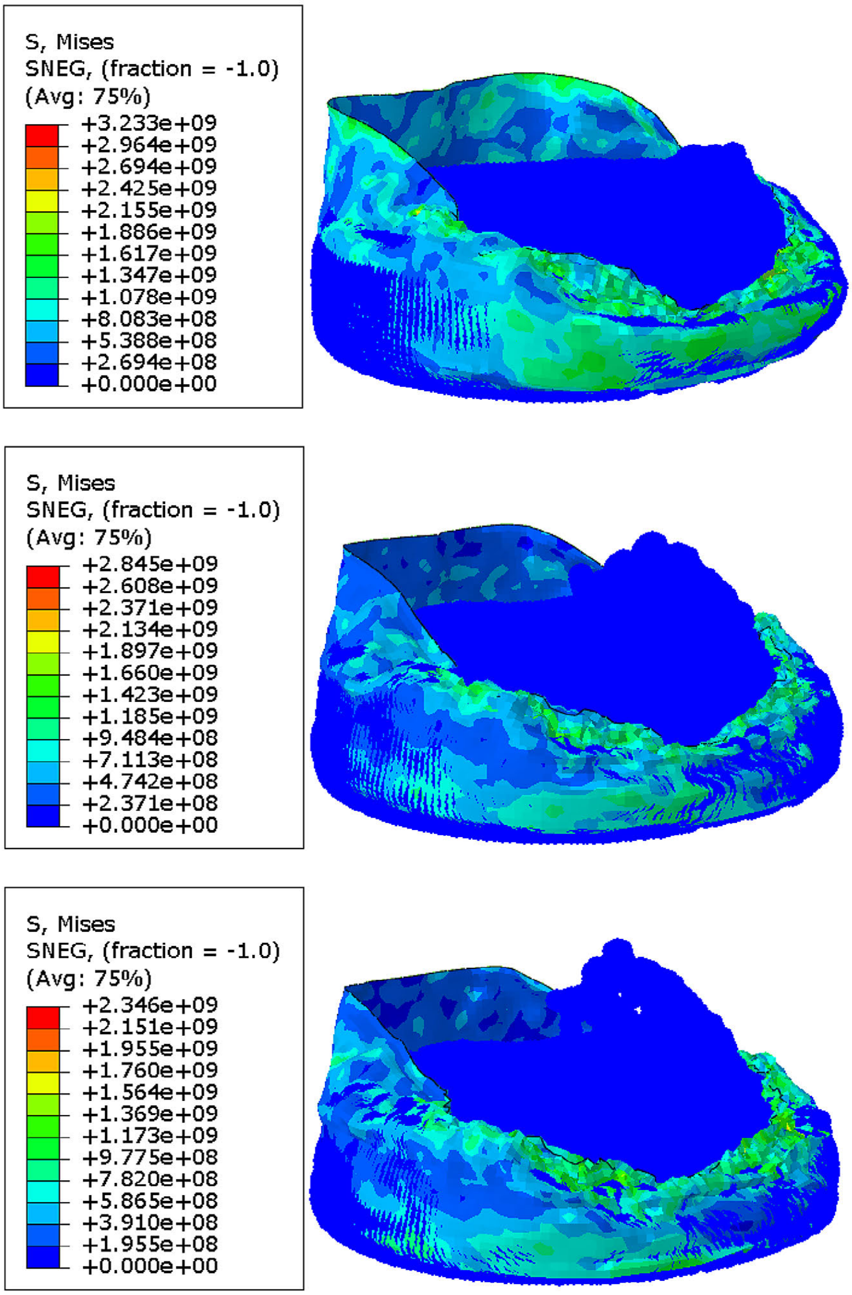

Figure 12. Cont. Von Mises stress distributed in V_3 model

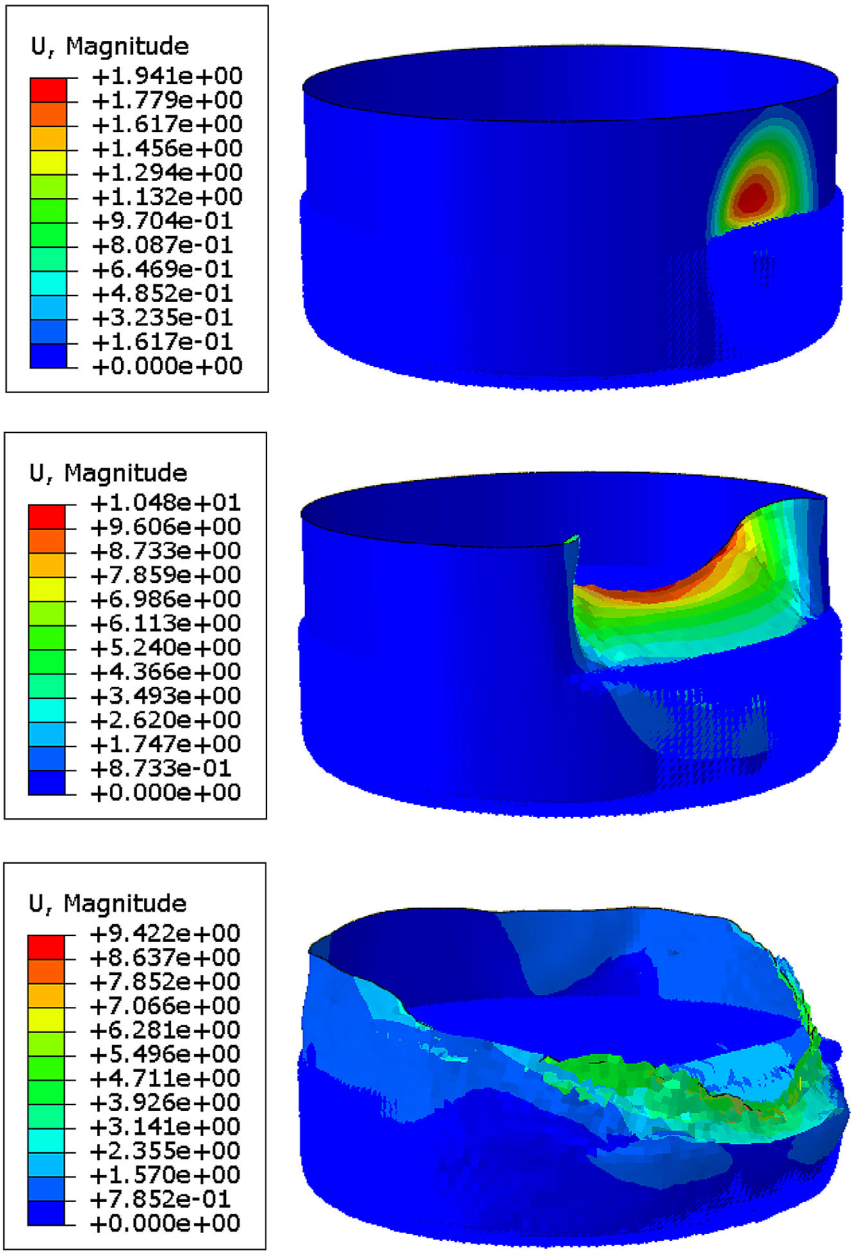

Figure 13. Displacement created in V_3 model

distance of the explosive material from the tank. In the first state, the distance of the explosive material from the tank is 25 m and in the second one, the distance is 10 m. In the both cases in this section, the cross-section of the tank is circular and the amount of the explosive material is 500 kg. Figures 6 and 16 show the distributed stress in V_1 and V_4 models respectively. The only difference of these two models is the distance of the explosive materials from the RC tank. As it can be seen, by reducing the distance of the explosive material from the tank, a significant increase in the tension created in the tank wall will occur. The maximum stress in V_1 and V_4 models are 590 MPa and 1021 MPa respectively. Therefore, when decreasing the distance of the explosives from the tank by 15 m, the maximum stress created in the RC tank will be increased by 42.2%. In other words, a 60% reduction of the distance will increase the maximum stress created in the tank by 42.2%.

Figures 7 and 17 show the maximum displacement of V_1 and V_4 models respectively. As it can be observed, by reducing the distance of the explosive material from the tank by 60%, a 9.9% increase will occur in the maximum displacement created in the concrete tank. Thus, the maximum displacement created in V_1 and V_4 models is 7.5 mm and 8.33 mm respectively.

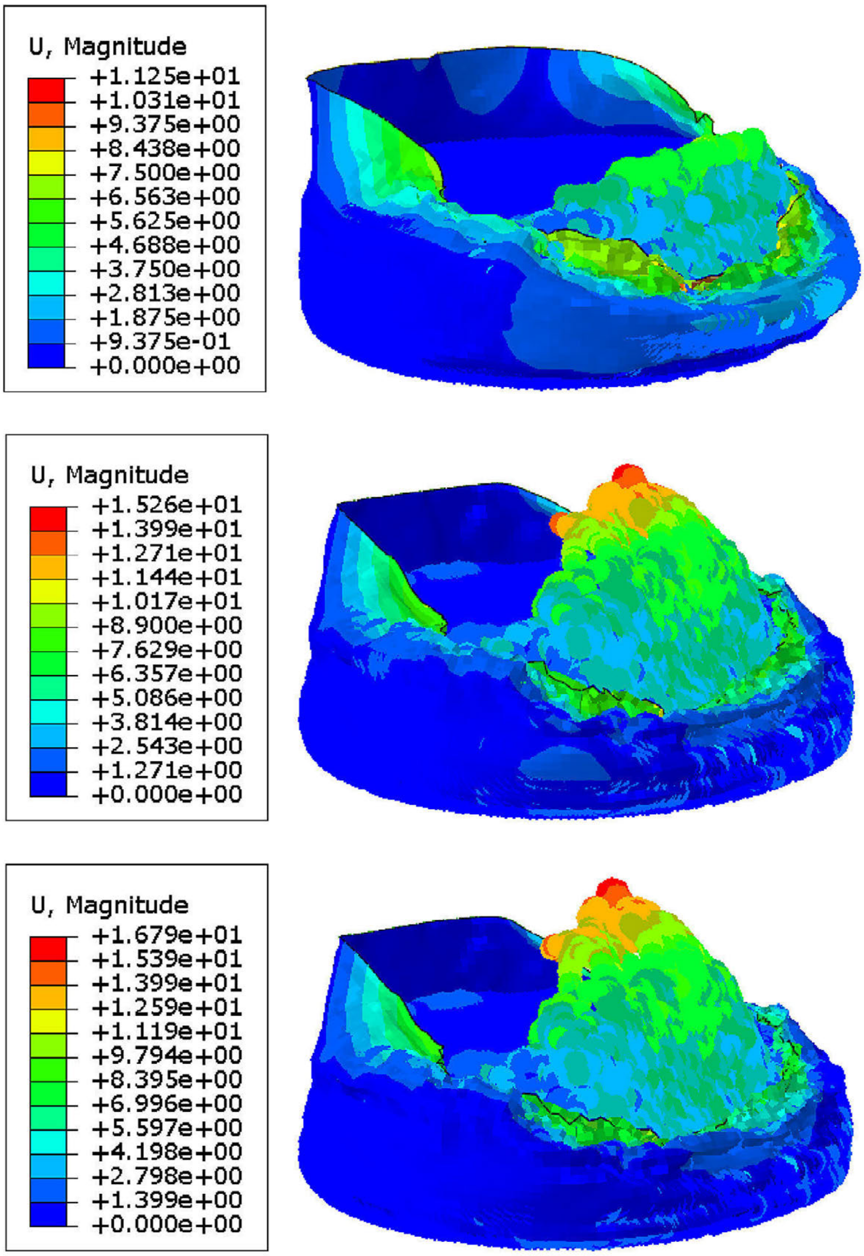

Figure 13. Cont. Displacement created in V_3 model

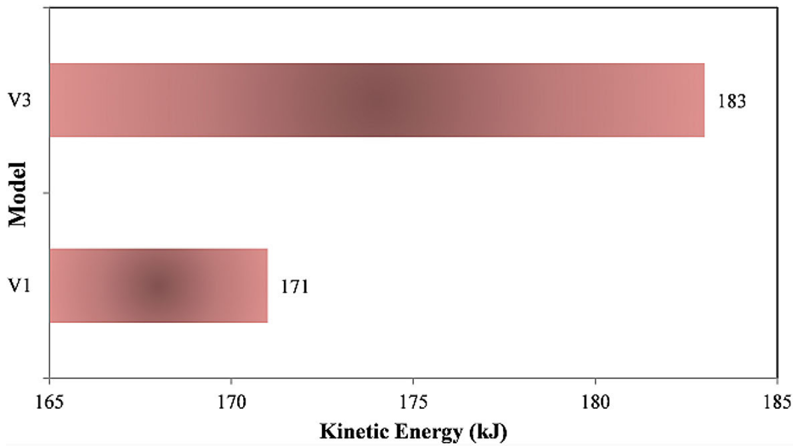

Figure 14. Effect of amount of explosive material on the kinetic energy response of the tank

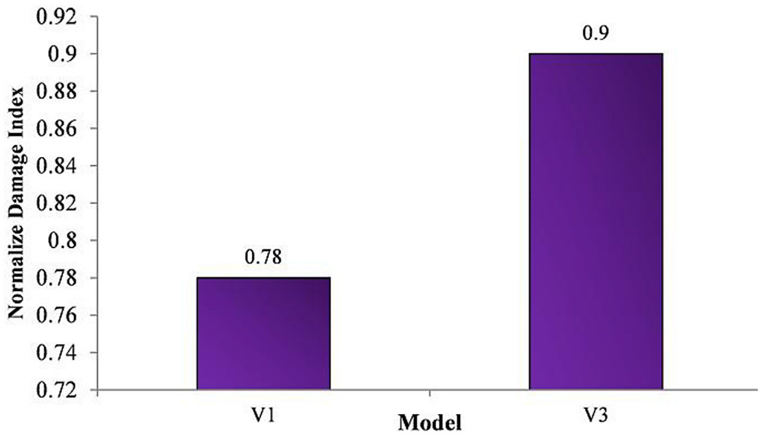

Figure 15. Effect of explosive material amount on failure index

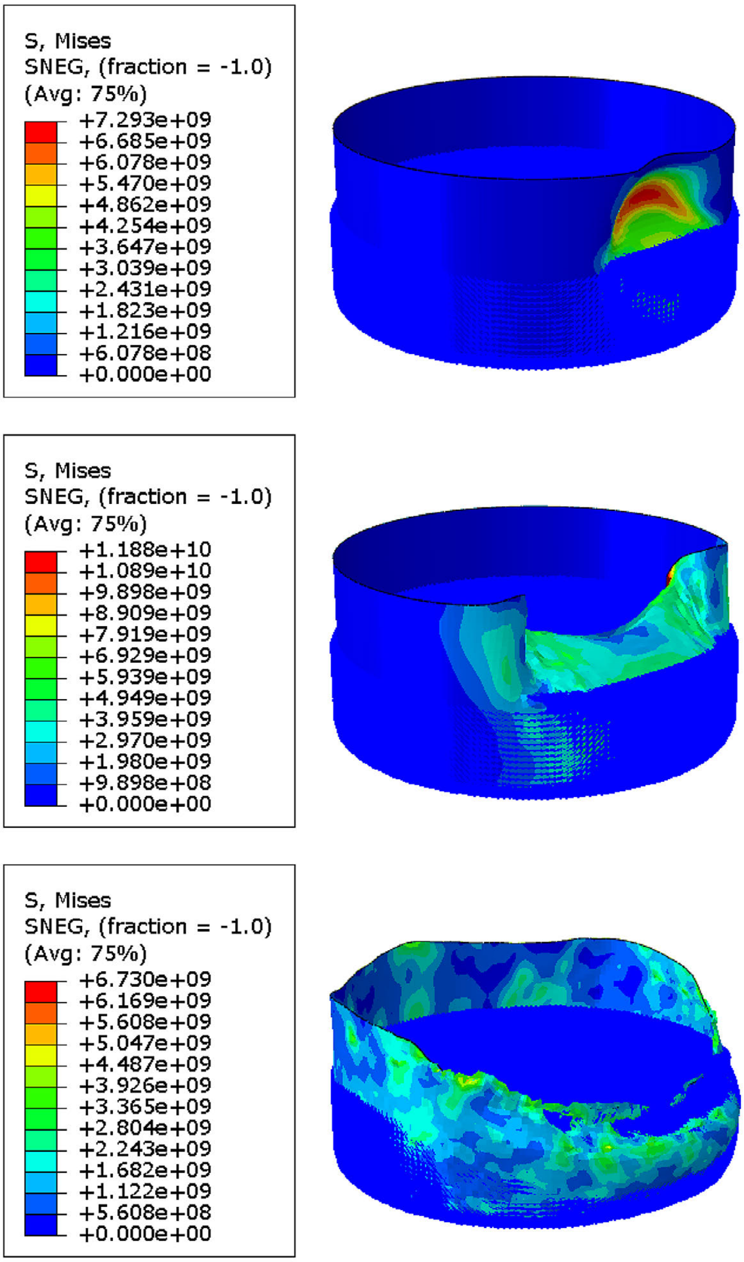

Figure 16. Von Mises stress distributed in V_4 model

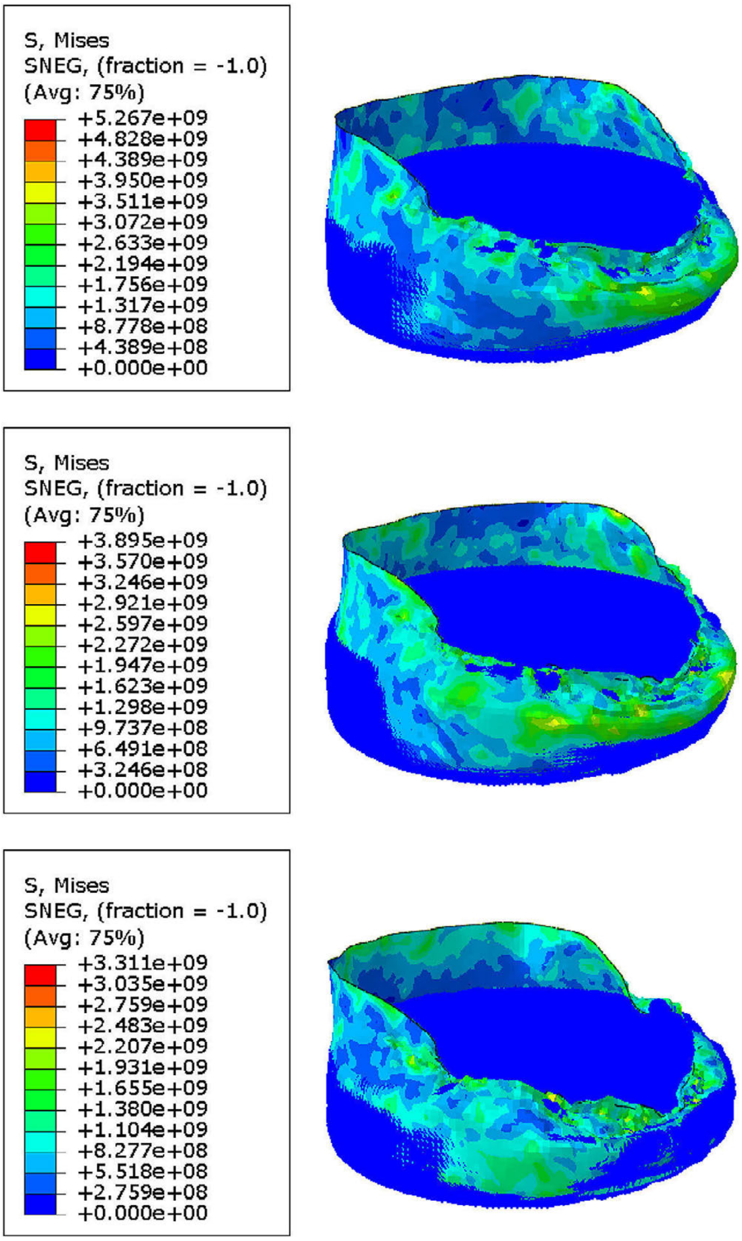

Figure 16. Cont. Von Mises stress distributed in V_4 model

Therefore, based on the presented results, by reducing the distance of the explosive material from 25 m to 10 m, the maximum displacement of the RC tank will be increased by 9.9%. Figure 18 shows the kinetic energy recorded in V_1 and V_4 models. With a 60% decrease in the distance of the TNT explosive from the tank, the amount of kinetic energy in the tank shows an increase of 8.16%. In other words, when the explosive material is located at the distance of 25 m (V_1 model) and 10m (V_4 model) from the tank, the kinetic energy in the tank will be 171 kJ and 186.2 kJ respectively. In order to determine the failure index, Park-Ang failure index is used in this case too. Figure 19 shows the failure index of V_1 and V_4 models. It can be seen that failure index of V_4 is 8.23% more than V_1. In other words, with a 60% reduce of the distance of explosive material from the tank, the probability of damaging and failure of the tank will be increased by 8.23%.

CONCLUSIONS

On the basis of the analysis carried out in this study, the results can be summarized as follows:

- by changing the cross-section of the tank from circular to square, the maximum stress

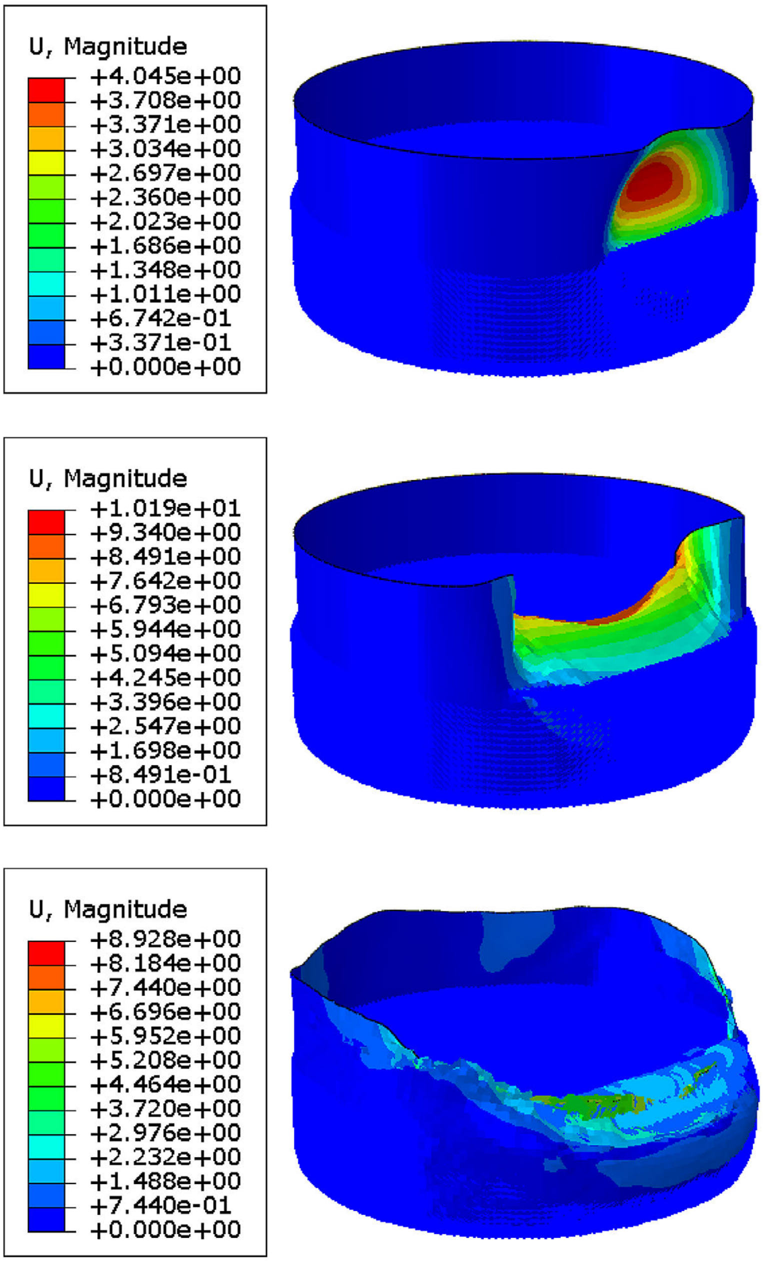

Figure 17. The displacement created in V_4 model

distributed in the tank will be increased by 9.1%. It can be justified due to the stress concentration formed in the corners of the square section.

- by increasing the amount of explosive material, the maximum stress distributed in the wall of the RC tank increased by 33%.
- by reducing the distance of the explosive material from the tank, the maximum stress distributed in the tank wall will be increased by 42.2%.
- by changing the cross-section of the tank from circular to square, the maximum displacement created in the tank will be increased by 35.9%.
- with the increase of the amount of explosive material, the maximum displacement created in the wall of the RC tank was increased by 44.4%.
- by reducing the distance of the explosive material from the tank, the maximum displacement created in the tank wall will be increased by 9.96%.
- by changing the cross-section of the tank from circular to square, the kinetic energy created in the tank will be decreased by 6.43%.
- with the increase of the amount of the explosive material, the kinetic energy created in the wall of the RC tank increased by 6.55%.

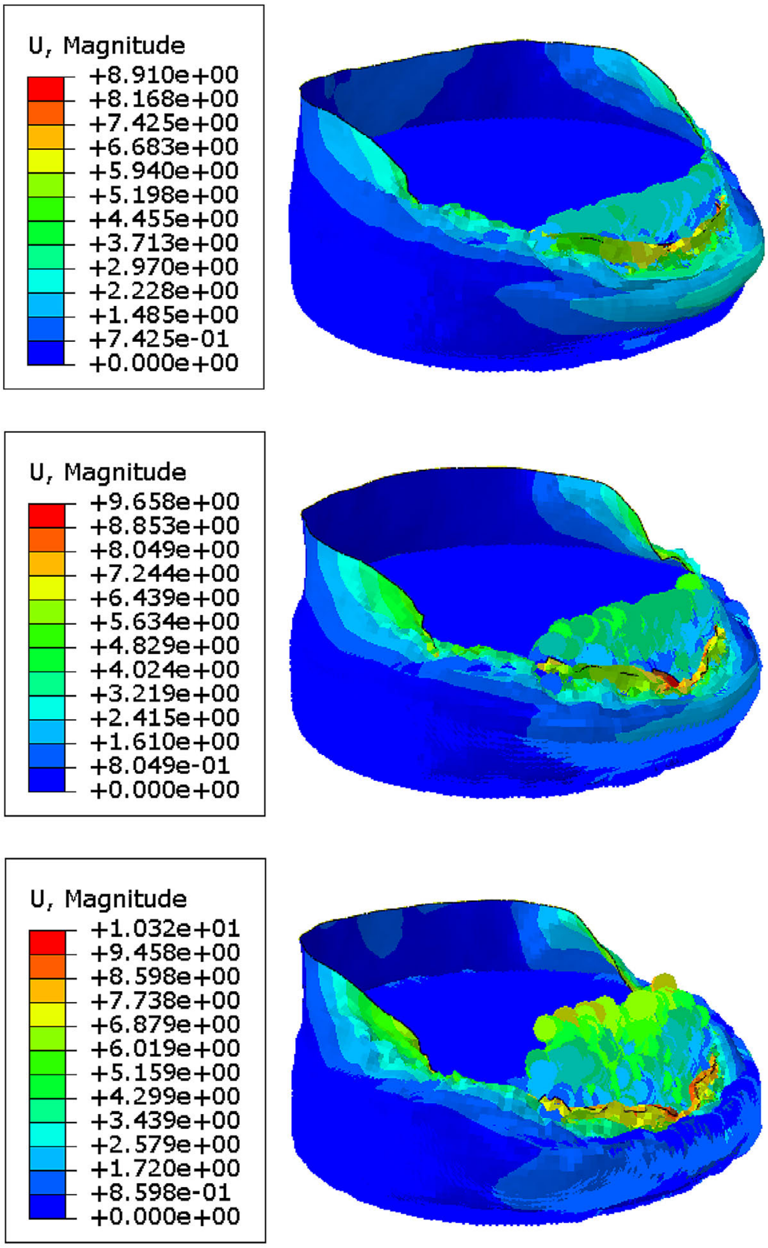

Figure 17. Cont. The displacement created in V_4 model

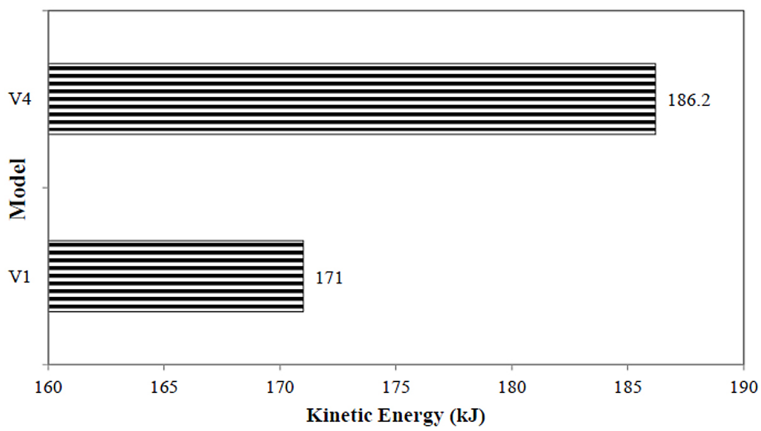

Figure 18. Effect of explosive material distance on kinetic energy response of the tank

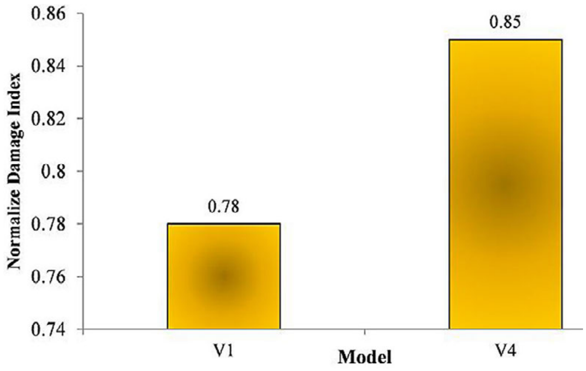

Figure 19. Effect of explosive material distance on failure index

- by reducing the distance of the explosive material from the tank, the kinetic energy created in the tank will be increased by 8.16%.
- by changing the cross-section of the tank from circular to square, the failure index of the tank will be increased by 3.7%.
- with the increase of the amount of explosive material, the failure index in the tank wall increased by 13.3%.
- by reducing the distance of the explosive material from the tank, the failure index in the tank wall will be increased by 8.23%.

REFERENCES

1. Housner, G. W. The dynamic behavior of water tanks. Bull Seismol Soc Am; 1963; 53(2): 381–7.
2. Rawat, A., Matsagar, V. A., and Nagpal, A. K. Numerical study of base-isolated cylindrical liquid storage tanks using coupled acoustic-structural approach. Soil Dynamics and Earthquake Engineering, 2019; 119, 196–219.
3. Khanmohammadi, M., Akhsvan Hejazi, F., and Hataminia, H. Investigation of the basics of design of concrete water tanks in different code. 2014. 8th National Congress on Civil Engineering, Babol.
4. Zou, D. Explosives. In Theory and Technology of Rock Excavation for Civil Engineering. 2017; 105–170.
5. Epstin, H. I. Seismic design of liquid storage tanks. J. Struct. Division, 1976; 102: 1673–1659.
6. Ghaemmaghami, A. R., Kianoush, M. R. Effect of wall flexibility on dynamic response of concrete rectangular tanks under horizontal and vertical ground motions. Journal of Structure Engineering, 2010; 136(4), 441–451.
7. Kianoush, M. R., Ghaemmaghami, A. R. The Effect of earthquake frequency content on the seismic behavior of concrete liquid tanks using the finite element method incorporating soil-structure interaction. Engineering Structure, 2011; 33(7): 2186–2200.
8. Khoshmoud, A., Alizadeh, A., and Allahyari, A. Analysis of the sensitivity of retrofitting of buried concrete tanks and the effect of soil type and distance from the explosion site. 2014. 8th National Congress on Civil Engineering, Babol.
9. Lin, F., Li, H. Safety analysis of nuclear containment vessels subjected to strong earthquakes and subsequent tsunamis. Nuclear Engineering and Technology, 2017; 49(5): 1079–1089.
10. Safa, P., and Shabdiz, S. Investigating the effect of explosion on above-ground tanks with floating roof. Scientific Publication of Passive Defense, 2015; 6(1): 13–24.
11. Burkacki, D., and Robert, J. Experimental study on steel tank model using shaking table. Civil and Environmental Engineering Reports, 2014; 14(3): 37–47.
12. Wu, K. C., Li, B., and Tasi, K. C. Residual axial compression capacity of localized blast-damaged RC columns. International Journal of Impact Engineering, 2011; 38(1): 29–40.
13. Tabatabaiefar, H. R., and Massumi, A. A simplified method to determine seismic responses of reinforced concrete moment resisting building frames under influence of soil-structure interaction. Soil Dynamics and Earthquake Engineering, 2010; 30(11): 1259–1267.
14. Chen, J. K., and Kianoush, M. R. Seismic response of concrete rectangular tanks for liquid containing structures. Canadian Journal of Civil Engineering, 2005; 32: 739–752.
15. Kianoush, M. R., and Chen, J. k. Effect of vertical acceleration on response of concrete rec tanks. Engineering Structure, 2006; 28(5): 704–7015.
16. Santoso, A. K., and Saito, T. An investigation of dynamic soil-structure interaction on the seismic behavior of RC base-isolated buildings. Civil Engineering Journal, 2024; 10(11): 3455–3472.
17. Li, S., and Shen, L. Seismic optimization design and application of civil engineering structures integrated with building robot system technology. High-tech And Innovation Journal, 2024; 5(4): 1118–1134.
18. Baumbach, M. R. Design of metal hollow section tubular columns subjected to transverse blast loads. Thin-Walled Structures, 2013; 68: 92–105.